Supporting Information

Supramolecular Engineering of Azelaic Acid-Nicotinamide Cocrystals for Dual Anti-Inflammatory and Brightening Efficacy

Experiment Section

1. Synthesis and characterization

1.1 Materials

[AzA], [Nic] and phosphate-buffered saline (PBS) were purchased from Aladdin Biochemical Technology Co. Ltd. (Shanghai, China). A Cell Counting Kit-8 (CCK-8), H&E staining kit, ROS assay kit, and SOD assay kit were acquired from Beyotime Biotechnology (Shanghai, China). HaCaT and MCF-7 cells were obtained from Bingcure Biotechnology Co. Ltd. (Wuhan, China). Dulbecco's Modified Eagle's medium (DMEM) was obtained from Gibco (Shanghai, China). TNF-α, IL-8, and PGE2 ELISA kits were purchased from Abcam (Shanghai, China). All organic solvents were of analytical purity, and all reagents were used as received.

1.2 Synthesis of [AzA][Nic]

4 mM [AzA] was slowly added to a 60 mL ethanolic solution of 4 mM [Nic], followed by stirring to achieve homogeneity. Subsequent reaction progression involved continuous stirring for 24 hours at 60 °C within a nitrogen (N_2) environment. Precipitated [AzA][Nic] crystals were harvested using rotary evaporation, subjected to cold ethanol washes, and dried under vacuum at 40 °C for 24 hours. The final single-crystal formation was accomplished by slow recrystallization from ethanol.

1.3 General characterization of [AzA][Nic]

Powder X-ray diffraction (XRD) patterns were recorded using a Rigaku D/max 2500PC instrument (Tokyo, Japan). Morphological characterization was performed via scanning electron

microscopy (SEM) using a Hitachi SU8010 system (Tokyo, Japan). Nuclear magnetic resonance (NMR) spectra were recorded at 400 MHz on a Bruker Avance Neo spectrometer (Fällanden, Switzerland) using deuterated dimethyl sulfoxide as the solvent. Infrared spectra were acquired in transmission mode using a Thermo Nicolet 380 FTIR spectrometer (Madison, WI, USA). Thermal stability (T_d) was determined using thermogravimetric analysis (PerkinElmer TGA 8000, Waltham, MA, USA). Melting point (T_m) was measured using differential scanning calorimetry (DSC, Mettler Toledo DSC3, Schwerzenbach, Switzerland). The crystal structure of [AzA][Nic] was determined using single-crystal X-ray diffraction (Agilent SuperNova, Dual, Cu at zero, AtlasS2 diffractometer, Palo Alto, CA, USA) and analyzed using the Olex2 program with the hydrogen atoms located from difference Fourier maps.

1.4 Water solubilities

The saturation shake-flask method was employed to determine aqueous solubilities. For each analyte, a concentration-absorbance calibration curve was constructed from UV-Vis measurements (PerkinElmer Lambda 365, USA) of serial dilutions. To prepare saturated solutions, an excess of sample was introduced into deionized water, subjected to 30 min of ultrasonication, and equilibrated under constant stirring for 48 h. After filtration to obtain a particle-free solution, solubility was quantified by applying the measured absorbance to its corresponding calibration curve.

2. Cellular efficacy evaluation

Cytotoxicity profiling was performed per SN/T 2328-2009 guidelines using MTT assays on human keratinocytes (HaCaT) and melanocytes (HMCs). Cultures with >90% cell viability were selected for subsequent experiments. Ultraviolet B (UVB) irradiation was used to induce cellular inflammation and oxidative stress. For ROS quantification, cells were rinsed thrice with PBS. ROS levels were assayed using a Beckman Coulter FC500 flow cytometer (Pasadena, CA, USA) according to the manufacturer's protocol. Following UVB exposure, cells were incubated 24 hours prior to biomarker assessment. SOD activity was measured in cell lysates, while TNF-α, IL-8, and PGE2 levels were quantified in cell culture supernatants, all according to specific kit instructions. Following treatment, human melanocytes were lysed. Lysate supernatant absorbances were measured at 405 nm using a microplate reader, and melanin content was quantified using a synthetic

melanin standard curve.

3. Computer simulations

DFT computations in this work were performed using the ORCA 5.0.4 program package, with structural optimizations at the B3LYP/6-31G* level and single-point energy calculations at the M06-2X/6-311++G** level.

A 3D PPARγ structure was acquired from the RCSB PDB database, and a ligand structure (SDF format) was retrieved from PubChem and converted to PDB format using OpenBabel. The target protein was prepared using AutoDock Tools 1.5.6 through dehydration and hydrogenation. Processed protein and ligand structures were converted to pdbqt format. Final docking simulations were performed within a defined binding site using AutoDock Vina.

Molecular dynamics (MD) simulations were performed using GROMACS 2020.3 software. The amber99sb-ildn force field and general Amber force field (GAFF) were used to generate the parameters and topologies of proteins and ligands, respectively. The primary objective of the simulation was to optimize the interaction between the target protein, solvent, and ions such that the simulation system was fully pre-equilibrated. All MD simulations were performed for 50 ns under an isothermal and isostatic ensemble at a temperature of 300 K and a pressure of 1 atm. Temperature and pressure were controlled using V-rescale and Parrinello-Rahman methods, respectively, and temperature and pressure coupling constants were 0.1 and 0.5 ps, respectively. The Lennard-Jones function was used to calculate the van der Waals force, and the nonbond truncation distance was set to 1.4 nm. The bond lengths of all atoms were constrained using the LINCS algorithm. The long-range electrostatic interactions were calculated using the Particle Mesh-Ewald method with a Fourier spacing of 0.16 nm.

4. Clinical trials

The study was conducted in accordance with the Declaration of Helsinki, approved by the Ethics Committee of Shinesky Testing Center (Project No. XJJC-S-2107005). Written informed consent was obtained from all participants prior to the study. Before efficacy test, an enclosed skin patch test was performed in accordance with the Cosmetic Safety Technical Specifications (2015 Edition) of China to ensure skin contact safety.

Skin colorimetric analysis: Under controlled conditions (22±1°C, RH 50±5%), healthy volunteers (Fitzpatrick III-IV, n≥30) acclimated for 30 min before measurements. Using Visial-CR, L (lightness), M (melanin index), ITA° (individual typology angle), and E (erythema index) values were recorded at baseline (D0) and at weeks 1, 2, 3, and 4. Five repeated measurements per test site were averaged with probe pressure <5 N. Efficacy was calculated as: $\Delta L = L_{(t)} - L_{(D0)}$; $\Delta M = M_{(D0)} - M_{(t)}$; $\Delta ITA° = ITA°_{(t)} - ITA°_{(D0)}$; $\Delta E = E_{(D0)} - E_{(t)}$. (Positive ΔL/ΔITA° and negative ΔM/ΔE indicate whitening/anti-redness effects).

5. Statistical analysis

Data are presented as means ± SD of ≥ 3 independent experiments. Statistical significance was assessed using GraphPad Prism 8.0, applying unpaired (cellular assays) or paired (clinical data) t-tests, with $p < 0.05$ considered significant.

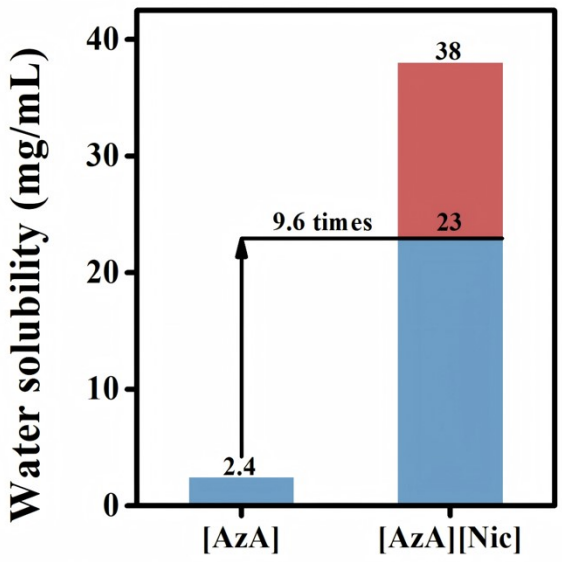

Fig. S1. Water solubilities of [AzA] and [AzA][Nic].

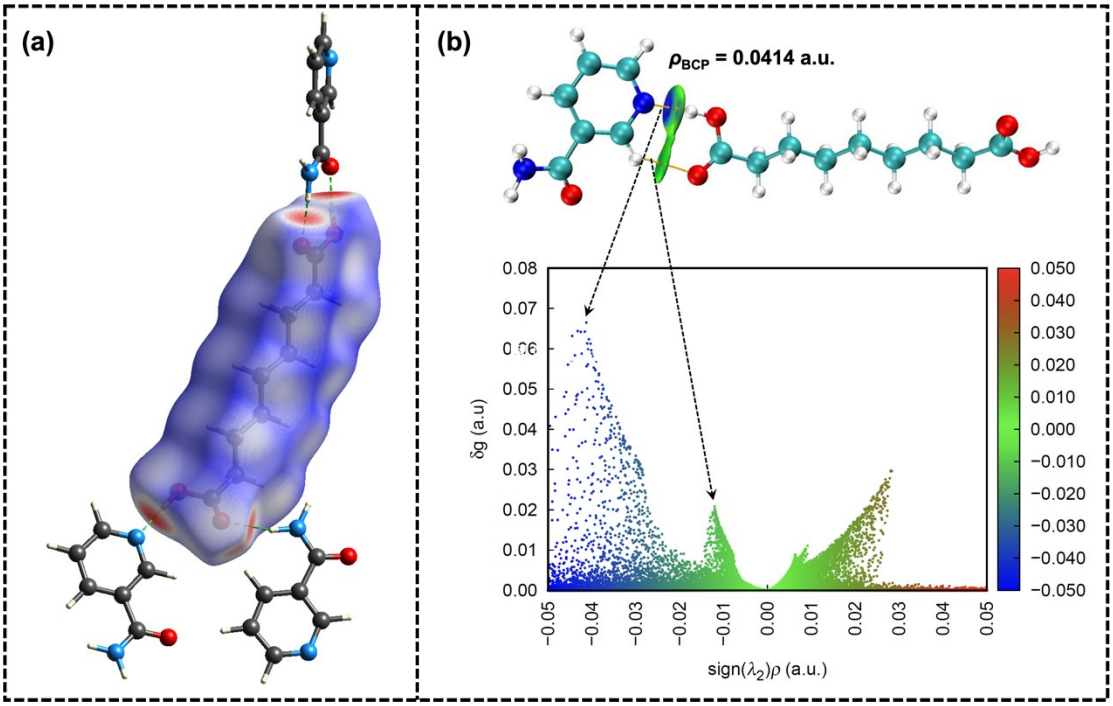

Fig. S2. Supramolecular interactions in [AzA][Nic]. (a) Analysis of 3D Hirshfeld dnorm surfaces for [AzA]. (c) Independent gradient model based on the Hirshfeld partition of molecular density (IGMH) of [AzA][Nic].

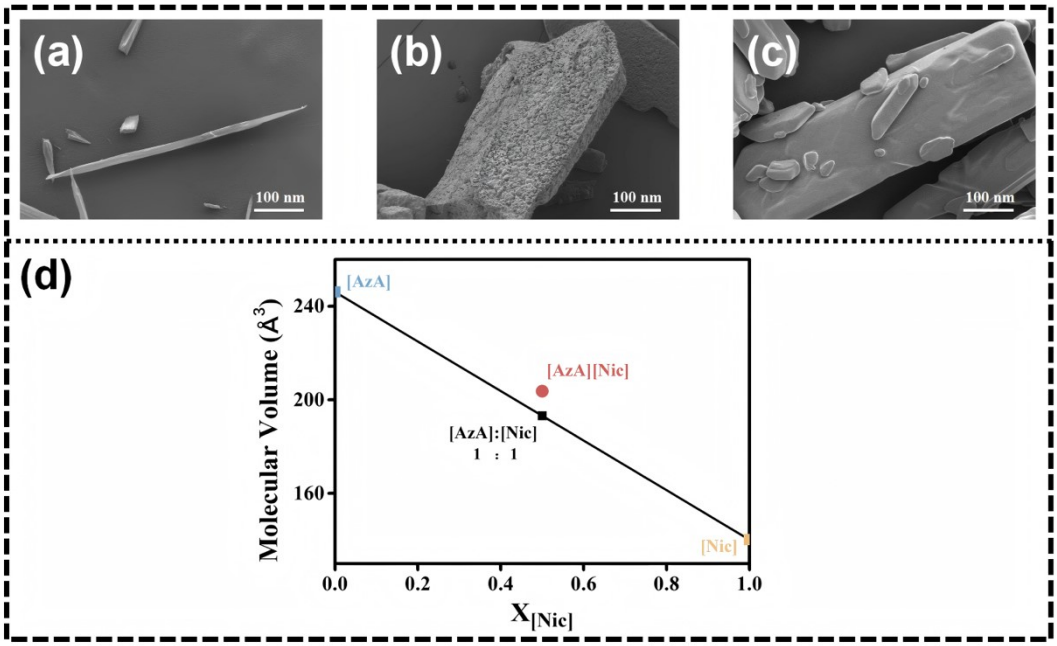

Fig. S3. SEM images of (a) [AzA], (b) [Nic], and (c) [AzA] [Nic]. (d) Comparison of weighted averages of the molecular volumes of the precursors with their cocrystal.

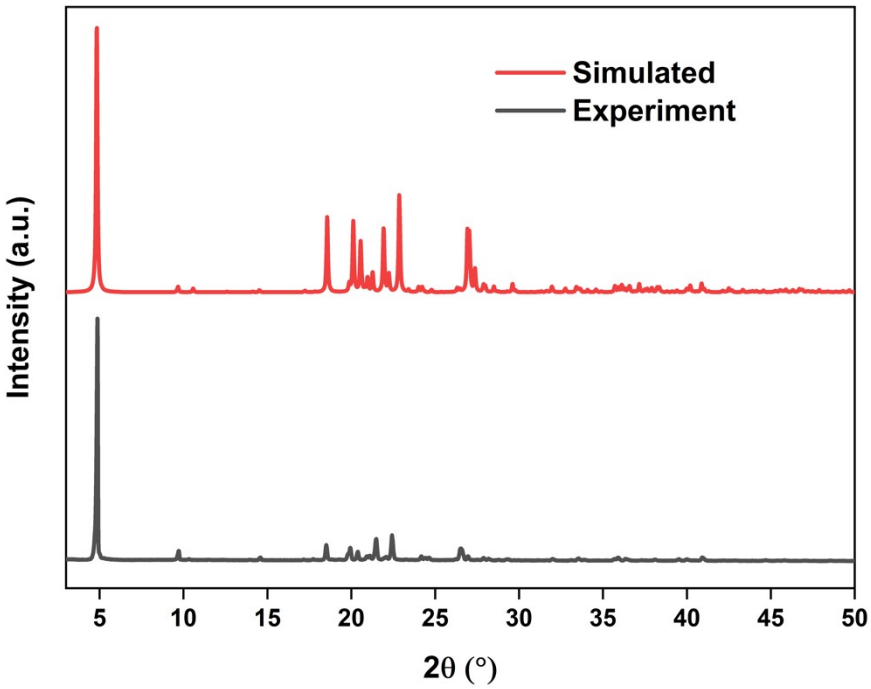

Fig. S4. The simulated XRD pattern from the single crystal data comparing to the powder XRD pattern.

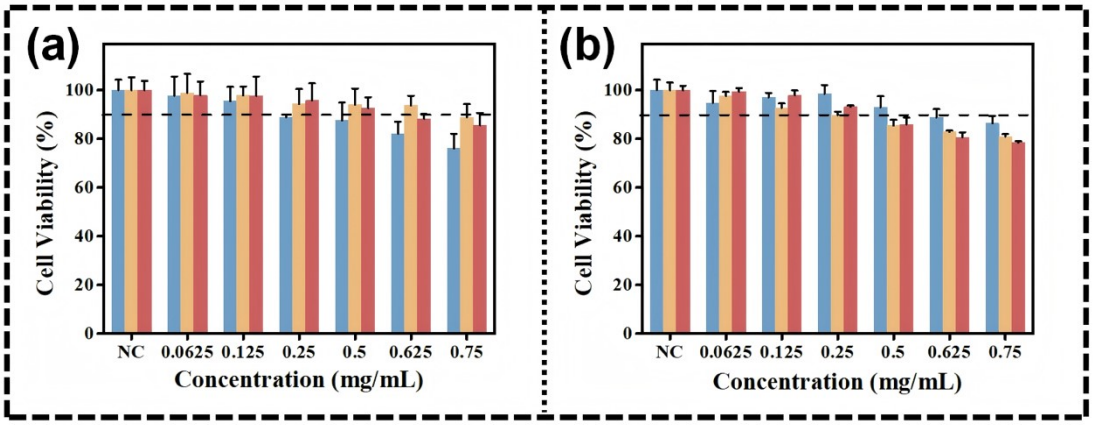

Fig. S5. Cytotoxicity of [AzA], [Nic], and [AzA][Nic] in (a) HaCaT cells and (b) HMCs.

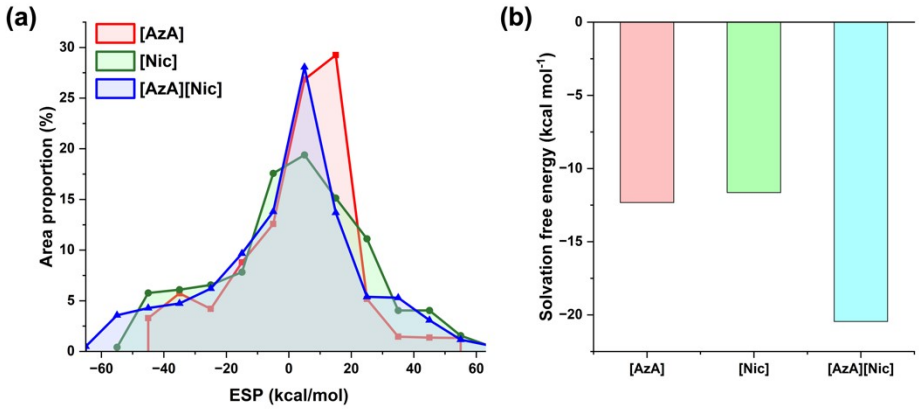

Fig. S6. (a) ESP distribution and (b) solvation free energies of [AzA], [Nic], and [AzA][Nic].

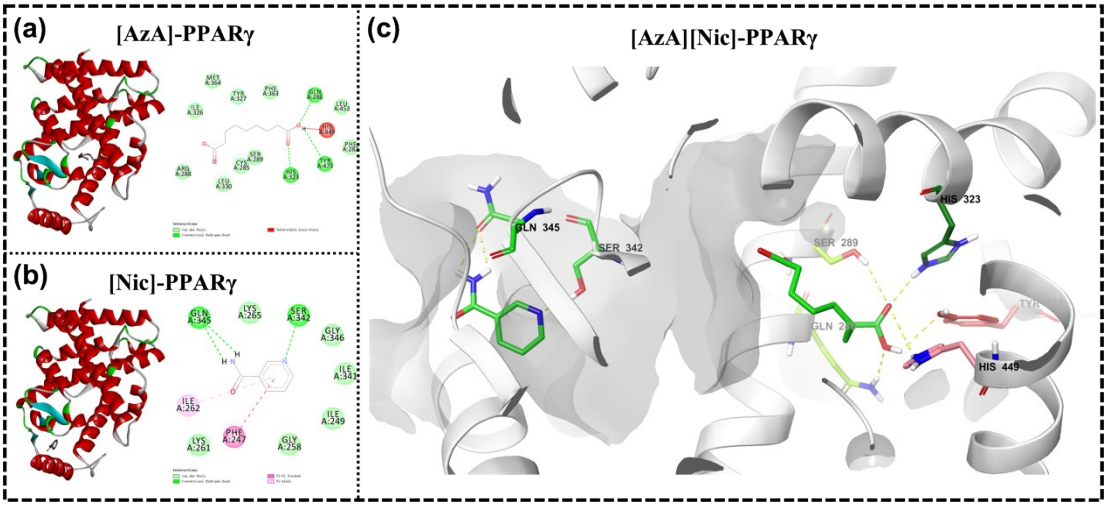

Fig. S7. The initial structures of MD simulations. (a) [AzA]-PPARγ (the optimized docking result with a binding energy of -4.9 Kcal/mol). (b) [Nic]-PPARγ (the optimized docking result with a binding energy of -4.7 Kcal/mol). (c) [AzA][Nic]-PPARγ (combination of the optimized docking results of [AzA]-PPARγ and [Nic]-PPARγ)

Table S1. Some reported AzA cocrystals

Coformer	AzA:Coformer (mol)	Tm (˚C)	Td (˚C)	Density (g/cm^3)	AzA Solubility (mg/mL)	Bioactivity	Ref.
Isonicotinamide	1:1	142	—	1.283	—	—	[1, 2]
Abacavir	1:2	153.8	—	1.280	2.67	—	[3]
Lidocaine	≤ 1:2	40-50	< 200	1.156*	—	—	[4]
Nicotinamide	1:1	113.99	228.28	1.265	23	Anti-oxidant Anti-inflammatory Whitening	This work

*For AzA: Lidocaine = 1:2 (mol)

Table S2. Structure of [AzA][Nic] cocrystal.

Sample	[AzA][Nic]
Empirical formula	$C_{15}H_{22}N_2O_5$
Formula weight	310.34
Temperature/K	150.00(10)
Crystal system	orthorhombic
Space group	$Pna2_1$
a/Å	8.5881(19)
b/Å	36.553(7)
c/Å	5.1905(5)
α/°	90
β/°	90
γ/°	90
Volume/Å^3	1629.4(5)
Z	4
ρ_{calc}g/cm^3	1.265
μ/mm^{-1}	0.793
F(000)	664.0
Crystal size/mm^3	0.12 × 0.11 × 0.1
Radiation	Cu Kα (λ = 1.54184)
2Θ range for data collection/°	4.836 to 149.332
Index ranges	$-10 \le h \le 7$, $-42 \le k \le 45$, $-6 \le l \le 5$
Reflections collected	6335
Independent reflections	2534 [R_{int}= 0.0735, R_{sigma}= 0.0689]
Data/restraints/parameters	2534/130/202
Goodness-of-fit on F^2	1.078
Final R indexes [I>=2σ (I)]	R_1= 0.0894, wR_2= 0.2239
Final R indexes [all data]	R_1= 0.1174, wR_2= 0.2505
Largest diff. peak/hole / e Å^{-3}	0.27/-0.32
Flack parameter	0.1(5)

Table S3. Torsion Angles for [AzA][Nic].

A	B	C	D	Angle/°	A	B	C	D	Angle/°
O1	C1	C2	C3	-170.8(4)	C10	N1	C14	C13	1.1(6)
O2	C1	C2	C3	13.2(7)	C10	C11	C12	C13	0.7(6)
C1	C2	C3	C4	-178.6(4)	C11	C12	C13	C14	1.2(6)
C2	C3	C4	C5	-178.2(4)	C11	C12	C13	C15	179.5(4)
C3	C4	C5	C6	-176.8(4)	C12	C13	C14	N1	-2.1(6)
C4	C5	C6	C7	178.3(4)	C12	C13	C15	O5	174.0(4)
C5	C6	C7	C8	179.2(4)	C12	C13	C15	N2	-8.9(6)
C6	C7	C8	C9	175.7(4)	C14	N1	C10	C11	0.9(6)
C7	C8	C9	O3	-111.3(5)	C14	C13	C15	O5	-7.7(6)
C7	C8	C9	O4	68.5(5)	C14	C13	C15	N2	169.4(4)
N1	C10	C11	C12	-1.8(6)	C15	C13	C14	N1	179.5(4)

Table S4. HOMO and LUMO energies of [AzA], [Nic] and [AzA][Nic].

Sample	HOMO/eV	LUMO/eV	Eg/eV
[AzA]	-9.803	0.123	9.926
[Nic]	-8.908	-0.788	8.120
[AzA][Nic]	-9.000	-0.841	8.159

Table S5. The calculated Bond Dissociation Enthalpy (BDE)、Ionization Potential (IP)、Proton Dissociation Enthalpy (PDE)、Proton Affinity (PA), and Electron Transfer Enthalpy (ETE) of [AzA], [Nic] and [AzA][Nic] (unit: kcal/mol).

Mechanism		HAT	SET-PT		SPLET	
		BDE	IP	PDE	PA	ETE
[AzA]		125.10	165.52	0.03	38.16	127.40
[Nic]		124.18	166.98	-2.35	54.44	110.19
[AzA][Nic]	H4	124.24	138.44	26.25	37.83	126.86
	H1	160.23		63.72	39.40	163.51
	H2C	124.41		27.90	54.47	112.62
	H2D	124.44		27.93	53.12	114.00

Table S6. The calculated binding free energies.

Energy	[AzA]	[Nic]	[AzA][Nic]
Van der Waals Energy (KJ/mol)	-12.745	-101.945	-209.411
Electrostatic energy (KJ/mol)	-12.745	4.487	-7.816
Polar solvation energy (KJ/mol)	51.588	19.843	86.749
Nonpolar solvation Energy(KJ/mol)	-15.590	-11.344	-23.036
Total Binding Energy(KJ/mol)	-101.623	-88.959	-153.514

Table S7. Composition table of 3 wt% [AzA][Nic] essence.

Group	Composition
[AzA][Nic] essence	water, glycerolpolyeter-26, glycerol glucoside, **[AzA][Nic],** glycerol, glycerol octanoate, octahydroxamic acid, 1.2-pentanediol, hydrolyzed small nucleusfungus gum, p-hydroxyacetophenone, disodium EDTA, Xanthan gum, sodium hyaluronate, sodium phenylbenzimidazole sulfonate, butanol polyeter-3, tributyl citrate, tri (tetramethylpiperidinol) titrate
Blank essence	Replace [AzA][Nic] with an equal amount of water and adjust the pH with NaOH (consistent with [AzA][Nic] essay)

Table S8. Grading criteria for skin reactions in skin sealing patch test.

Extent	Grade	Skin reactions
-	0	Negative reaction.
±	1	Suspicious reaction: only weak erythema.
+	2	Weak positive reaction (erythema reaction): erythema, infiltration, edema, possiblae papules.
++	3	Strong positive reaction (herpes reaction): erythema, infiltration, edema, papules, herpes, reaction may extend beyond the test area.
+++	4	Extremely strong positive reaction (fusion herpes reaction): obvious erythema, severe infiltration, edema, fusion herpes, reaction beyond the test area.

Table S9. Summary of results of human skin patch test.

Group	Number of participants	Observation time	Number of people with different levels of skin reactions				
			0	**1**	**2**	**3**	**4**
[AzA][Nic] essence	30	0.5 h	30	0	0	0	0
		24 h	30	0	0	0	0
		48 h	30	0	0	0	0
Blank essence	30	0.5 h	30	0	0	0	0
		24 h	30	0	0	0	0
		48 h	30	0	0	0	0
Negative control (Blank + Filter)	30	0.5 h	30	0	0	0	0
		24 h	30	0	0	0	0
		48 h	30	0	0	0	0

Among the 30 subjects, no adverse reactions occurred, indicating that the above kinds of essence had low irritation and basically did not cause irritation to human skin, so they could be safely used in daily chemical products.

Supplementary References

(1) Thompson, L. J.; Voguri, R. S.; Male, L.; Tremayne, M. The crystal structures and melting point properties of isonicotinamide cocrystals with alkanediacids HO2C(CH2)n-2CO2H n=7-9. *Crystengcomm* **2011**, *13* (12), 4188-4195.

(2) Yarava, J. R.; Potnuru, L. R.; Pahari, B.; Tothadi, S.; Ramanathan, K. V. Supramolecular Synthon Identification in Azelaic Acid - Isonicotinamide. *J. Magn. Reson. Open* **2022**, *10-11*.

(3) Ji, X.; Wu, D.; Li, C.; Li, J. L.; Sun, Q.; Chang, D. W.; Yin, Q. X.; Zhou, L. N.; Xie, C.; Gong, J. B.; et al. Enhanced Solubility, Dissolution, and Permeability of Abacavir by Salt and Cocrystal Formation. *Crystal Growth & Design* **2022**, *22* (1), 428-440.

(4) Zotova, J.; Wojnarowska, Z.; Twamley, B.; Tajber, L. Formation of stoichiometric and non-stoichiometric ionic liquid and cocrystal multicomponent phases of lidocaine with azelaic acid by changing counterion ratios. *J. Mol. Liq.* **2021**, *344*, 117737.